Progress in Fractional Differentiation and Applications
An International Journal

http://dx.doi.org/10.18576/pfda/100302

Numerical Approximation of Fractional Order Transmission of Worms in Wireless Sensor Network in Sense of Caputo Operator

Amita Devi[1], *Aziz Khan*[2], *Anoop Kumar*[1,*], *Thabet Abdeljawad*[2,*]

[1] Department of Mathematics and Statistics, Central University of Punjab, Bathinda, Punjab, India
[2] Department of Mathematics and General Sciences, Prince Sultan University, P.O. Box 66833, 11586 Riyadh, Saudi Arabia

Received: 29 May 2022, Revised: 9 Jun 2022, Accepted: 10 Jun. 2022
Published online: 1 Jul. 2024

Abstract: In this manuscript, we study the uncertain attacking of some worms in wireless sensor network (WSNs). We established a mathematical formulation for the WSNs model in the sense of Caputo fractional operator. Applying the fixed point theory, certain theoretic solutions of existence and uniqueness are considered for the fractional model. In addition, to investigate reproduction number, local stability and Hyers-Ulam stability of the proposed model. Furthermore, Corrector-Predictor algorithm is utilized for fractional dynamics and numerical solutions.

Keywords: Fractional-order model, wireless sensor network, Ulam-Hyers stability, Krasnoselkii fixed point, local stability.

1 Introduction, motivation and preliminaries

A computer worm is a self-reprodusing program that is able to spread and copy itself without the help of any other program. Worms use a software or operating system to replicate itself, relying on security holes or policy flaws on the target software or operating systems to access it, such as the instinctive file receiving and sending attributes found on many devices. It will use this device as a host to scan and infect the other machine. It can replicate itself very rapidly. Thus, continuous replication and infection of this virus to other software programs can be harmfull for the computer users. A worm can control and infect more and more machines in a short time. Moreover, new type viruses are continuously created WSNs have obtained considerable attention because of their large number of applications in earthquake measurements to warfare, military and civil areas [1]. The sensor nodes are alluring targets for software attacks.The reliability and unification of the computer and WSNs is in danger due to the cyber attack by worm. Computer worms are also a type of computer virus, but there are some aspects that differenciate computer worms from regular viruses. A main dissimilarity is the fact that viruses propagate through human activity as opening a file, running a program, etc while computer worms can replicate itself without human initiation [2,3,4] . Recently, the new type of worms exposure have seen which especially targets movable devices, for instance laptops, mobile, etc. The new characteristic of these worms is that the internet connection is not required for their replication. They can propagate itself through wireless network technology, such as Private hotspot, Bluetooth or Wi-Fi [5,6]. The more use of malicious code to transfer large number of unnecessary email for profit is also a thereat for WSNs. The model SEIR analysed by Yan and Liu [7] presumes that the recovery hosts acuire permanent immunity which is not compatible with real state. In order to avoid this condition, a SEIRS model with immune and latent periods proposed by Mishra and Saini [8], which can disclose common worm replication. In last few years, fusion of virus propagation and is became a hot research topic for instance, quarantine [9,10,11] and virus immunization [12,13,14].The replicating dynamics of a mobile sensor worm and local defending strategy to recover the network is propagated from the microscopic point of view by Wang et al. [15]. The epidemic behavior and the effect of digital worms with node distributed density and different communication radius by Akansha et al.[16]. They analysed the

* Corresponding author e-mail: anoop.kumar@cup.edu.in, tabdeljawad@psu.edu.sa

usefulness of epidemic model to transfering the data in WSNs and also studied the stability theory of proposed model. The random jammming attacks can target media access control (MAC)/link layers and physical condition of all nodes in a WSNss, nevertheless computing power of the machines. The effect of theses random jammming attacks in WSNs is studied by Mishra et al. [17]. To study the effect of energy conservation in the situation of worm attacks in WSNs a model on predator–prey dynamics is proposed by Mishra and Keshri[18]. They also established different equilibrium points for stability conditions. The spread of worms of the type of PLC-PC a mathematical model is proposed by Yao et al.[19] in ICS network and this model also can be used to explain the interaction between different defense strategies and worm epidemics. The existence and local stability of endemic equilibrium of Hopf bifurcation is established by Zhang et al.[20] by using the center manifold theorem and normal form theory. An optimal control approach is used to reduce the propagation of malware in WSNs. The node-based epidemic modeling technique is used to study the malware trace-patch model with geometrical boundaries for sensors by Muthukrishnan et al. [21]. The effect of the MAC apparatus on virus replication in WSNs with limited communication capacity and uniform random distribution based on the Waxman algorithm is studied by Jiang et al.[22]. Ganeshan and Selvan [23] discussed the analytical solution for the WSNs model by using the Homotopy Perturbation Method. The solution of network access control model involving fractional derivative is established with help of fractional natural decomposition method by Ilhan [24]. An optimal control strategy is used to control the propegation of the virus and dynamic analysis of SEIR model is discussed by Liu et al. [25] with the help of the Pontryagin maximum principle. The EU of soution is established with technique of contraction principle for fuzzy fractional SIQR worm propagation WSNs model involving Caputo Atangana-Baleanu derivatives by Dong et al. [26]. The different type of fractional differential equations and fractional order model under different conditions has been analysed widely [27,28,29,30,31,32]. An epidemic model which express the generation dynamics of worm and consumption of sensor nodes energy because of worm attack is proposed by Awasthi et al.[33]. The charging method of sensor nodes and consumption of energy by sensor nodes due to worms attack in WSNs is discussed in this model.

Motivated by the above mention work, in this article, we describe the uncertain attacking nature of some worms in WSNs. The proposed mathematical model advances the existing integer-order model on possible worms in WSNs. We solve the projected model for analyzing the dynamical behaviour of worms propagation within the frame of Caputo fractional derivative. The projected model can boost anti-virus power of the network and permit the system to modify elasticity to various worms by initiating a preservation tool in the sleep nodes of WSNs. As in the cyber world immunization is not permanent, the nodes are temporarily resistant and subsequently become susceptible towards the attainable attack of worms. The EU of the solutions of the proposed model is analysed using the fixed point theorems. The projected model will be significant to outline and examine the fact for WSNs and communication network. So the fractional-order model presented in (1) is as follows:

$$\begin{cases} {}^{c}\mathcal{D}^{\omega}\mathcal{S} = \mathcal{A} - \beta\mathcal{S}\mathcal{I} - \mu\mathcal{S} - p\mathcal{S} + \delta\mathcal{R} + \eta\mathcal{V} \qquad t \in [0,\mathcal{b}], \\ {}^{c}\mathcal{D}^{\omega}\mathcal{E} = \beta\mathcal{S}\mathcal{I} - (\mu+\alpha)\mathcal{E} \\ {}^{c}\mathcal{D}^{\omega}\mathcal{I} = \alpha\mathcal{E} - (\mu+\varepsilon+\gamma)\mathcal{I} \\ {}^{c}\mathcal{D}^{\omega}\mathcal{R} = \gamma\mathcal{I} - (\mu+\delta)\mathcal{R} \\ {}^{c}\mathcal{D}^{\omega}\mathcal{V} = p\mathcal{S} - (\mu+\eta)\mathcal{V} \end{cases} \tag{1}$$

with initial conditions

$$\mathcal{S}(0) = \mathcal{S}_0 \geq 0;\ \ \mathcal{I}(0) = \mathcal{I}_0 \geq 0;\ \ \ \mathcal{E}(0) = \mathcal{E}_0 \geq 0;\ \ \ \mathcal{R}(0) = \mathcal{R}_0 \geq 0;\ \ \ \mathcal{V}(0) = \mathcal{V}_0 \geq 0 \ \text{ and } \ t \in [0,b],\ \ b \in \mathbb{R}^{+}.$$

The operator ${}^{c}\mathcal{D}^{\omega}$ denotes the Caputo fractional-order derivative of order $0 \leq \omega < 1$. At time t, $\mathcal{S}(t)$ denote the number of susceptible, $\mathcal{E}(t)$ represent the exposed nodes, infectious are represented by $\mathcal{I}(t)$, $\mathcal{R}(t)$ are recovered nodes and $\mathcal{V}(t)$ is the number of vaccinated nodes. Also assume that $\mathcal{N} = \mathcal{S} + \mathcal{E} + \mathcal{I} + \mathcal{R} + \mathcal{V}$.

Description of model parameters Description of parameters involved in model (1) is given in the following table:

Now,

$${}^{c}\mathcal{D}^{\omega}\mathcal{N} = \mathcal{A} - \mu\mathcal{N} - \varepsilon\mathcal{I}.$$

If we avoid attacks, then number of node approaches the transferring proportions $\frac{\mathcal{A}}{\mu}$. The fractional differential equation for $\mathcal{N}$ gives the solution of (1) in region $\mathfrak{N}$, where

$$\mathfrak{N} = \{(\mathcal{S},\mathcal{E},\mathcal{I},\mathcal{R},\mathcal{V}) : \mathcal{S} \geq 0, \mathcal{E} \geq 0, \mathcal{I} \geq 0, \mathcal{R} \geq 0, \mathcal{V} \geq 0,\ \mathcal{S}+\mathcal{E}+\mathcal{I}+\mathcal{R}+\mathcal{V} \leq \frac{\mathcal{A}}{\mu}\}.$$

Table 1: Description of Parameters involved in model (1).

Parameter	Description
$\mathcal{A}$	is the involvement of new sensor nodes to the population,
γ	is the recovery rate,
p	is the rate coefficient of vaccination for the susceptible nodes,
ε	the crashing rate due to attack of worms,
η	represent the rate of transmission from $\mathcal{V}$-class to $\mathcal{S}$-class,
β	denotes the infectivity contact rate,
δ	is the transfering rate from $\mathcal{R}$-class to $\mathcal{S}$-class,
μ	is the rate of crash of the sensor nodes because of hardware/software problem,
α	is the rate of transmission from $\mathcal{E}$-class to $\mathcal{I}$-class,

This article is arranged as: Section 2^{nd} discusses the essential preliminaries and some important results. In the next section, we establish the EU results of the model (1). Section 4^{th} and Section 5^{th} are devoted to examining the local and Ulam-Hyers stability of the model (1) using the concept of basic reproduction number $\mathcal{R}_0$ and Ulam-Hyers stability criteria, respectively. In the final analysis, we perform numerical simulations using the Corrector-Predictor algorithm and discuss obtained results with the help of graphs.

2 Auxiliary results

Here, we offer desired lemmas, theorems and some definitions, which are important in obtaining the existence of solutions.
Definition 2.1.[34] For a function $\theta^* : (0,+\infty) \longrightarrow \mathbb{R}$, Riemann-Liouville integral of fractional order $\delta > 0$ is defined as

$$I^{\delta}\theta^*(t) = \frac{1}{\Gamma(\delta)}\int_0^t (t-\nu)^{\delta-1}\theta^*(\nu)d\nu, \quad \delta > 0,$$

provided, that right side of the above equation is pointwise defined on$(0,+\infty)$.

Definition 2.2.[34] For real valued function $\theta^* : (0,+\infty) \longrightarrow \mathbb{R}$, the Caputo's derivative of fractional order $\delta \in \mathbb{R}$ $(\delta > 0)$, is defined as

$${}^{c}\mathcal{D}^{\delta}\theta^*(t) = \frac{1}{\Gamma(\mathsf{m}-\delta)}\int_0^t (t-\nu)^{\mathsf{m}-\delta-1}(\theta^*)^{\mathsf{m}}(\nu)d\nu, \quad \mathsf{m}-1 < \delta < \mathsf{m}, \quad \mathsf{m} = [\delta]+1,$$

where integral exist on $(0,+\infty)$ and $[\delta]$ represent the greatest-integer, provided that θ^* is m-times continuously differentiable on $(0,+\infty)$.
Lemma 2.1.[35] Let $\theta^*(t) \in C^{m-1}$ and $\kappa \in (m-1,m]$, then

$$\mathcal{I}^{\kappa}\mathcal{D}^{\kappa}\theta^*(\nu) = \theta^*(\nu) + a_0 + a_1\nu + a_2\nu^2 + a_3\nu^3 + ... + a_{m-1}\nu^{m-1},$$

for the $a_j \in \mathbb{R}$ where $j = 0,1,2,...,m-1$.

Lemma 2.2.[36]**Generalized Mean Value Theorem**: Let $f(t) \in C[a,b]$ and $\mathcal{D}_t^{\omega}f(t) \in (a,b]$. Then for $0 < \omega \leq 1$,

$$f(t) - f(a) = \frac{1}{\Gamma(\omega)}\mathcal{D}_t^{\omega}f(\eta)(t-a)^{\omega}, \ \ 0 \leq \eta \leq t, \forall t \in (a,b].$$

Theorem 2.1. (Krasnoselkii Fixed Point Theorem)[37] Let $\mathcal{S}$ is a nonempty, closed, bounded and convex subset of a Banach space E. Let A_1, A_2 be the operators from $\mathcal{S}$ to E such that:
(i) $A_1x + A_2y \in \mathcal{S}$ whenever $x, y \in \mathcal{S}$;
(ii) A_1 is continuous and compact;
(iii) A_2 is a contraction map.
Then there exists $\mathfrak{z} \in \mathcal{S}$ such that $\mathfrak{z} = A_1\mathfrak{z} + A_2\mathfrak{z}$.

3 Existence of solutions

Here we establish the EU result of model (1) with help of fixed point theorems. Let us reformulated the system (1) in compact form for easy description. Let

$$\aleph(t) = [\mathcal{S}(t), \mathcal{E}(t), \mathcal{I}(t), \mathcal{R}(t), \mathcal{V}(t)]^T \quad \text{and}$$
$$\mathcal{H}\big(t, \aleph(t)\big) = [\Psi_1(t, \aleph(t)), \Psi_2(t, \aleph(t)), \Psi_3(t, \aleph(t)), \Psi_4(t, \aleph(t)), \Psi_5(t, \aleph(t))]^T,$$

where

$$\begin{aligned}
\Psi_1(t, \aleph(t)) &= \mathcal{A} - \beta \mathcal{S}\mathcal{I} - \mu\mathcal{S} - p\mathcal{S} + \delta\mathcal{R} + \eta\mathcal{V} \\
\Psi_2(t, \aleph(t)) &= \beta \mathcal{S}\mathcal{I} - (\mu + \alpha)\mathcal{E} \\
\Psi_3(t, \aleph(t)) &= \alpha\mathcal{E} - (\mu + \varepsilon + \gamma)\mathcal{I} \\
\Psi_4(t, \aleph(t)) &= \gamma\mathcal{I} - (\mu + \delta)\mathcal{R} \\
\Psi_5(t, \aleph(t)) &= p\mathcal{S} - (\mu + \eta)\mathcal{V}
\end{aligned}$$

So the dynamical system of equation (1) can be write as:

$${}^{c}\mathcal{D}^{\omega}\aleph(t) = \mathcal{H}\big(t, \aleph(t)\big); \quad \aleph(0) = \aleph_0 \geq 0, \quad t \in [0, b], \quad 0 < \omega \leq 1. \tag{2}$$

Applying the integral operator I^{ω} on equation (3). Then equation (3) is equivalent to the integral equation

$$\aleph(t) = \aleph_0 + \frac{1}{\Gamma(\omega)} \int_0^t (t - \varsigma)^{\omega - 1} \mathcal{H}\big(\varsigma, \aleph(\varsigma)\big) d\varsigma. \tag{3}$$

Lemma 3.1. The function $\mathcal{H}\big(t, \aleph(t)\big)$ defined above satisfies

$$|\mathcal{H}(t, \aleph) - \mathcal{H}(t, \bar{\aleph})| \leq \mathcal{L}_{\mathcal{H}} |\aleph - \bar{\aleph}|, \qquad t \in [0, b],$$

for some $\mathcal{L}_{\mathcal{H}} \geq 0$.
Proof. By the definition of function $\mathcal{H}\big(t, \aleph(t)\big)$,

$$\|\mathcal{H}\big(t, \aleph(t)\big) - \mathcal{H}\big(t, \bar{\aleph}(t)\big)\| = \sup_{t \in [0,b]} \sum_{i=1}^{5} \Big|\Psi_i(t, \aleph(t)) - \Psi_i(t, \bar{\aleph}(t))\Big| \tag{4}$$

First we find the,

$$\Big|\Psi_i(t, \aleph(t)) - \Psi_i(t, \bar{\aleph}(t))\Big| \leq \beta |\mathcal{S}\mathcal{I} - \bar{\mathcal{S}}\bar{\mathcal{I}}| + (\mu + p)|\mathcal{S} - \bar{\mathcal{S}}| + \delta|\mathcal{R} - \bar{\mathcal{R}}| + \eta|\mathcal{V} - \bar{\mathcal{V}}| \tag{5}$$

However

$$\begin{aligned}
|\mathcal{S}\mathcal{I} - \bar{\mathcal{S}}\bar{\mathcal{I}}| &= |\mathcal{S}\mathcal{I} - \bar{\mathcal{S}}\bar{\mathcal{I}} - \mathcal{S}\bar{\mathcal{I}} + \mathcal{S}\bar{\mathcal{I}}| \\
&\leq f_1|\mathcal{I} - \bar{\mathcal{I}}| + f_2|\mathcal{S} - \bar{\mathcal{S}}|
\end{aligned}$$

with $f_1 = \sup_{t \in [0,b]} |\mathcal{S}(t)|$ and $f_2 = \sup_{t \in [0,b]} |\bar{\mathcal{I}}(t)|$
Therefore Equ. (5) implies that

$$\begin{aligned}
\Big|\Psi_1(t, \aleph(t)) - \Psi_1(t, \bar{\aleph}(t))\Big| &\leq \beta\big(f_1|\mathcal{I} - \bar{\mathcal{I}}| + f_2|\mathcal{S} - \bar{\mathcal{S}}|\big) + (\mu + p)|\mathcal{S} - \bar{\mathcal{S}}| + \delta|\mathcal{R} - \bar{\mathcal{R}}| + \eta|\mathcal{V} - \bar{\mathcal{V}}| \\
&\leq \big(\beta f_2 + \mu + p\big)|\mathcal{S} - \bar{\mathcal{S}}| + \beta f_1|\mathcal{I} - \bar{\mathcal{I}}| + \delta|\mathcal{R} - \bar{\mathcal{R}}| + \eta|\mathcal{V} - \bar{\mathcal{V}}|.
\end{aligned}$$

$$\Big|\Psi_1(t, \aleph(t)) - \Psi_1(t, \bar{\aleph}(t))\Big| \leq \mathcal{L}_1\Big(|\mathcal{S} - \bar{\mathcal{S}}| + |\mathcal{I} - \bar{\mathcal{I}}| + |\mathcal{R} - \bar{\mathcal{R}}| + |\mathcal{V} - \bar{\mathcal{V}}|\Big),$$

where,

$$\mathcal{L}_1 = \sup_{t \in [0,b]} \Big\{\beta f_1 + \beta f_2\Big\} + \mu + p + \delta + \eta.$$

Similarly,

$$\begin{aligned}
&\left|\Psi_2(t,\aleph(t))-\Psi_2(t,\bar{\aleph}(t))\right| \le \mathcal{L}_2\Big(|\mathcal{S}-\bar{\mathcal{S}}|+|\mathcal{I}-\bar{\mathcal{I}}|+|\mathcal{E}-\bar{\mathcal{E}}|\Big);\\
&\left|\Psi_3(t,\aleph(t))-\Psi_3(t,\bar{\aleph}(t))\right| \le \mathcal{L}_3\Big(|\mathcal{I}-\bar{\mathcal{I}}|+|\mathcal{E}-\bar{\mathcal{E}}|\Big);\\
&\left|\Psi_4(t,\aleph(t))-\Psi_4(t,\bar{\aleph}(t))\right| \le \mathcal{L}_4\Big(|\mathcal{I}-\bar{\mathcal{I}}|+|\mathcal{R}-\bar{\mathcal{R}}|\Big);\\
&\left|\Psi_5(t,\aleph(t))-\Psi_5(t,\bar{\aleph}(t))\right| \le \mathcal{L}_5\Big(|\mathcal{S}-\bar{\mathcal{S}}|+|\mathcal{V}-\bar{\mathcal{V}}|\Big);
\end{aligned}$$

where,

$$\begin{aligned}
\mathcal{L}_2 &= \sup_{t\in[0,b]}\Big\{\beta f_1+\beta f_2\Big\}+\mu+\alpha;\\
\mathcal{L}_3 &= \mu+\varepsilon+\gamma+\alpha;\\
\mathcal{L}_4 &= \mu+\delta+\gamma;\\
\mathcal{L}_5 &= \mu+\eta+\rho.
\end{aligned}$$

Consequently,

$$\begin{aligned}
\|\mathcal{H}\big(t,\aleph(t)\big)-\mathcal{H}\big(t,\bar{\aleph}(t)\big)\| &= \sup_{t\in[0,b]}\big\{\mathcal{L}_1+\mathcal{L}_2+\mathcal{L}_3+\mathcal{L}_4+\mathcal{L}_5\big\}\Big[|\mathcal{S}-\bar{\mathcal{S}}|+|\mathcal{E}-\bar{\mathcal{E}}|\\
&\quad+|\mathcal{I}-\bar{\mathcal{I}}|+|\mathcal{R}-\bar{\mathcal{R}}|+|\mathcal{V}-\bar{\mathcal{V}}|\Big]\\
&\le \mathcal{L}_{\mathcal{H}}\|\aleph-\bar{\aleph}\|,
\end{aligned}$$

with $\mathcal{L}_{\mathcal{H}}=\mathcal{L}_1+\mathcal{L}_2+\mathcal{L}_3+\mathcal{L}_4+\mathcal{L}_5$.
This complete the proof.

Theorem 3.1. Let us consider that Lemma 3.1. holds. Then problem (1) has at least one solution defined on $\mathcal{I}=[0,b]$.

Proof We shall examine the model (1) in the form of integral equation. For this aim, let $\mathcal{X}=C\big([0,b],\mathbb{R}\big)$; $\mathcal{X}$ denote the Banach space of all functions from $[0,b]$ to $\mathbb{R}$, which are continuous and endowed with the norm

$$\|\aleph\|_{\mathcal{X}} = \sup_{t\in[0,b]}\{|\aleph(t)|\},$$

where

$$|\aleph(t)| = |\mathcal{S}(t)|+|\mathcal{E}(t)|+|\mathcal{I}(t)|+|\mathcal{R}(t)|+|\mathcal{V}(t)|.$$

Consider $\mathbb{B}_{\Omega}=\{\aleph : \|\aleph\|\le\Omega\}$ is closed, bounded and convex set with $\Omega \ge \dfrac{\|\aleph_0\|+\mathcal{H}_0\Lambda}{1-\mathcal{L}_{\mathcal{H}}\Lambda}$,

where $\Lambda=\dfrac{(b)^{\omega}}{\Gamma(\omega+1)}$.
Define an operator $\mathcal{F}:\mathcal{X}\longrightarrow\mathcal{X}$ as

$$\mathcal{F}\aleph(t) = \aleph_0+\frac{1}{\Gamma(\omega)}\int_0^t(t-\varsigma)^{\omega-1}\mathcal{H}\big(\varsigma,\aleph(\varsigma)\big)d\varsigma. \tag{6}$$

Also, define two operator $\mathcal{F}_1$and$\mathcal{F}_2$ as

$$\mathcal{F}_1\aleph(t)=\aleph_0, \qquad t\in\mathcal{I}.$$

$$\mathcal{F}_2\aleph(t)=\frac{1}{\Gamma(\omega)}\int_0^t(t-\varsigma)^{\omega-1}\mathcal{H}\big(\varsigma,\aleph(\varsigma)\big)d\varsigma.$$

Now we will show that operator $\mathcal{F}_1$ and $\mathcal{F}_2$ satisfy all requirements of Theorem 2.1. To achieve this goal we offer the proof in following steps as:

1.To prove $\mathcal{F}_1\aleph_1+\mathcal{F}_2\aleph_2\in\mathbb{B}_{\Omega}$.

$\|\mathcal{F}_1\aleph_1+\mathcal{F}_2\aleph_2\|\leq \Omega \quad$ where $\Omega\in\mathbb{B}_\Omega$,
For any $\aleph_1,\aleph_2\in\mathbb{B}_\Omega$

$$\begin{aligned}
&\|\mathcal{F}_1\aleph_1+\mathcal{F}_2\aleph_2\|\\
&\quad=\sup_{t\in[0,b]}\left\{\left|\aleph_0+\frac{1}{\Gamma(\omega)}\int_0^t(t-\varsigma)^{\omega-1}\mathcal{H}\big(\varsigma,\aleph_2(\varsigma)\big)\partial\varsigma\right|\right.\\
&\quad\leq\sup_{t\in[0,b]}\left\{|\aleph_0|+\frac{1}{\Gamma(\omega)}\int_0^t(t-\varsigma)^{\omega-1}\Big|\mathcal{H}\big(\varsigma,\aleph_2(\varsigma)-\mathcal{H}\big(\varsigma,\aleph_2(\varsigma)-\mathcal{H}\big(\varsigma,\aleph_2(\varsigma)\big)\Big|\partial\varsigma\right\}\\
&\quad\leq\|\aleph_0\|+\big(\mathcal{L}_{\mathcal{H}}\|\aleph_2\|+\mathcal{H}_0\big)\sup_{t\in[0,b]}\left\{\frac{1}{\Gamma(\omega)}\int_0^t(t-\varsigma)^{\omega-1}\partial\varsigma\right\}\\
&\quad\leq\|\aleph_0\|+\frac{\big(\mathcal{L}_{\mathcal{H}}\|\aleph_2\|+\mathcal{H}_0\big)}{\Gamma(\omega+1)}(b)^\omega\\
&\quad\leq\|\aleph_0\|+\frac{\big(\mathcal{L}_{\mathcal{H}}\Omega+\mathcal{H}_0\big)}{\Gamma(\omega+1)}(b)^\omega\\
&\quad\leq\Omega.
\end{aligned}$$

This confirms that $\mathcal{F}_1\aleph_1+\mathcal{F}_2\aleph_2\in\mathbb{B}_\Omega$.

It is obvious, $\mathcal{F}_1$ is contraction map.

2.We show that $\mathcal{F}_2$ is relatively compact.
To prove $\mathcal{F}_2$ is relatively compact. We show that $\mathcal{F}_2$ is continuous, uniform bounded and equicontinuous.
$\aleph(t)$ is continuous, then $\mathcal{F}_2\aleph(t)$ is continuous.
Next, $\aleph(t)\in\mathbb{B}_\Omega$, we have

$$\begin{aligned}
\|\mathcal{F}_2\aleph\|&=\sup_{t\in[0,b]}\left\{\left|\frac{1}{\Gamma(\omega)}\int_0^t(t-\varsigma)^{\omega-1}\mathcal{H}\big(\varsigma,\aleph(\varsigma)\big)\partial\varsigma\right|\right\}\\
&\leq\sup_{t\in[0,b]}\left\{\frac{1}{\Gamma(\omega)}\int_0^t(t-\varsigma)^{\omega-1}\Big|\mathcal{H}\big(\varsigma,\aleph(\varsigma)-\mathcal{H}\big(\varsigma,\aleph(\varsigma)-\mathcal{H}\big(\varsigma,\aleph(\varsigma)\big)\Big|\partial\varsigma\right\}\\
&\leq\big(\mathcal{L}_{\mathcal{H}}\|\aleph\|+\mathcal{H}_0\big)\sup_{t\in[0,b]}\left\{\frac{1}{\Gamma(\omega)}\int_0^t(t-\varsigma)^{\omega-1}\partial\varsigma\right\}\\
&\leq\frac{\big(\mathcal{L}_{\mathcal{H}}\|\aleph\|+\mathcal{H}_0\big)}{\Gamma(\omega+1)}(b)^\omega\\
&\leq\frac{\big(\mathcal{L}_{\mathcal{H}}\Omega+\mathcal{H}_0\big)}{\Gamma(\omega+1)}(b)^\omega\\
&<\infty.
\end{aligned}$$

which shows that $\mathcal{F}_2$ is bounded on $\mathbb{B}_\Omega$.
For any $0<t_1<t_2<t<1$, we have

$$\begin{aligned}
&\|\mathcal{F}_2\aleph(t_2)-\mathcal{F}_2\aleph(t_1)\|\\
&\quad\leq\frac{1}{\Gamma(\omega)}\int_{t_1}^{t_2}(t_2-\varsigma)^{\omega-1}\big|\mathcal{H}\big(\varsigma,\aleph(\varsigma)\big)\big|\partial\varsigma+\frac{1}{\Gamma(\omega)}\int_0^{t_1}(t_1-\varsigma)^{\omega-1}-(t_2-\varsigma)^{\omega-1}|\mathcal{H}\big(\varsigma,\aleph(\varsigma)\big)\big|\partial\varsigma\\
&\quad\leq\frac{\big(\mathcal{L}_{\mathcal{H}}\Omega+\mathcal{H}_0\big)}{\Gamma(\omega+1)}[(t_2-t_1)^\omega+(t_1^\omega-t_2^\omega)+(t_2-t_1)^\omega],
\end{aligned}$$

$\|\mathcal{F}_2\aleph(t_2)-\mathcal{F}_2\aleph(t_1)\|\longrightarrow 0$ as $t_2\longrightarrow t_1$. Consequently, $\mathcal{F}_2$ is equicontinuous operator on $\mathcal{B}_\Omega$. Therefore by the Arzela-Ascoli theorem $\mathcal{F}_2$ is relatively compact on $\mathcal{B}_\Omega$. Hence by theorem (2.1) $\mathcal{F}$ has at least one fixed point. Thus $\aleph$ is that fixed point of $\mathcal{F}$. Consequently, u is solution of equ. (1).

3.1 Uniqueness result

Here, we will investigate the uniqueness of solutions of equation (1). Then the problem (1) reduce to the second kind hybrid fractional differential equation

Theorem 3.2. Let us assume that *Lemma*(3.1) holds. Then the projected model (1) has unique solution on $[0,b]$, if

$$\mathcal{L}_{\mathcal{H}}\frac{(b)^{\omega}}{\Gamma(\omega+1)}=\mathcal{L}_{\mathcal{H}}\Lambda<1, \tag{7}$$

holds and $\mathcal{L}_{\mathcal{H}}=\mathcal{L}_1+\mathcal{L}_2+\mathcal{L}_3+\mathcal{L}_4+\mathcal{L}_5$.

Proof. Let the operator $\mathcal{F}:\mathcal{X}\longrightarrow\mathcal{X}$ defined by (6)

We show that $\mathcal{F}$ is uniform bounded operator. Next, $\aleph(t)\in\mathbb{B}_{\Omega}$, we have

$$\begin{aligned}
\|\mathcal{F}\aleph\| &= \sup_{t\in[0,b]}\left\{\left|\frac{1}{\Gamma(\omega)}\int_0^t(t-\varsigma)^{\omega-1}\mathcal{H}\big(\varsigma,\aleph(\varsigma)\big)d\varsigma\right|\right\}\\
&\leq \sup_{t\in[0,b]}\left\{\aleph_0+\frac{1}{\Gamma(\omega)}\int_0^t(t-\varsigma)^{\omega-1}\Big|\mathcal{H}\big(\varsigma,\aleph(\varsigma)-\mathcal{H}\big(\varsigma,\aleph(\varsigma)-\mathcal{H}\big(\varsigma,\aleph(\varsigma)\big)\Big|d\varsigma\right\}\\
&\leq \|\aleph_0\|+\big(\mathcal{L}_{\mathcal{H}}\|\aleph\|+\mathcal{H}_0\big)\sup_{t\in[0,b]}\left\{\frac{1}{\Gamma(\omega)}\int_0^t(t-\varsigma)^{\omega-1}d\varsigma\right\}\\
&\leq \aleph_0++\frac{\big(\mathcal{L}_{\mathcal{H}}\|\aleph\|+\mathcal{H}_0\big)}{\Gamma(\omega+1)}(b)^{\omega}\\
&\leq \aleph_0++\frac{\big(\mathcal{L}_{\mathcal{H}}\Omega+\mathcal{H}_0\big)}{\Gamma(\omega+1)}(b)^{\omega}\\
&< \infty.
\end{aligned}$$

which shows that $\mathcal{F}$ is bounded on $\mathbb{B}_{\Omega}$.

Next, we show that $\mathcal{F}$ is contraction map.

For each $\aleph,\aleph_1\in\mathcal{X}$ and using Lemma (3.1), we have

$$\begin{aligned}
\|\mathcal{F}\aleph_1-\mathcal{F}\aleph_2\| &= \sup_{t\in[0,b]}\left\{\left|\aleph_0+\frac{1}{\Gamma(\omega)}\int_0^t(t-\varsigma)^{\omega-1}\mathcal{H}\big(\varsigma,\aleph_1(\varsigma)\big)d\varsigma-\aleph_0-\frac{1}{\Gamma(\omega)}\int_0^t(t-\varsigma)^{\omega-1}\mathcal{H}\big(\varsigma,\aleph_2(\varsigma)\big)d\varsigma\right|\right\}\\
&\leq \sup_{t\in[0,b]}\left\{\frac{1}{\Gamma(\omega)}\int_0^t(t-\varsigma)^{\omega-1}\Big|\mathcal{H}\big(\varsigma,\aleph_1(\varsigma)-\mathcal{H}\big(\varsigma,\aleph_2(\varsigma)\big)\Big|d\varsigma\right\}\\
&\leq \big(\mathcal{L}_{\mathcal{H}}\|\aleph_1-\aleph_2\|\big)\sup_{t\in[0,b]}\left\{\frac{1}{\Gamma(\omega)}\int_0^t(t-\varsigma)^{\omega-1}d\varsigma\right\}\\
&\leq \mathcal{L}_{\mathcal{H}}\frac{(b)^{\omega}}{\Gamma(\omega+1)}\|\aleph_1-\aleph_2\|\\
&= \mathcal{L}_{\mathcal{H}}\Lambda\|\aleph_1-\aleph_2\|,
\end{aligned}$$

but in (7) assumed that $\mathcal{L}_{\mathcal{H}}=\mathcal{L}_1+\mathcal{L}_2+\mathcal{L}_3+\mathcal{L}_4+\mathcal{L}_5$. Hence by (7), $\mathcal{F}$ is contraction map. Consequently, Banach contraction mapping principle implies that $\mathcal{F}$ has a unique fixed point, which is unique solution for projected model 1.

4 Worm free equilibrium

For WFE, we have ${}^{c}\mathcal{D}^{\omega}\mathcal{S}=0$, ${}^{c}\mathcal{D}^{\omega}\mathcal{E}=0$, ${}^{c}\mathcal{D}^{\omega}\mathcal{I}=0$, ${}^{c}\mathcal{D}^{\omega}\mathcal{R}=0$ and ${}^{c}\mathcal{D}^{\omega}\mathcal{V}=0$ and after solving , we have WFE point as: $P=\left(\frac{\mathcal{A}(\mu+\eta)}{\mu(\mu+\eta+\rho)},0,0,0,\frac{\rho\mathcal{A}}{(\mu+\delta)(\mu+\rho)-\rho\eta}\right)$ for worm free state. Here we examine local asymptomatic stability of the disease model (1) with the help of basic reproduction number $\mathcal{R}_0$. The infected subsystem of model (1) can be written as

$${}^{c}\mathcal{D}^{\omega}\aleph=\mathsf{F}-\mathsf{V},$$

where,

$$\mathsf{F}=\begin{pmatrix}0&\beta\\0&0\end{pmatrix},$$

and

$$\mathsf{V} = \begin{pmatrix} \mu+\alpha & \beta \\ -\alpha & \mu+\varepsilon+\gamma \end{pmatrix}.$$

The basic reproduction number $\mathcal{R}_0$ is the largest eigen value of the matrix FV^{-1}. We compute FV^{-1} as:

$$\mathsf{FV}^{-1} = \begin{pmatrix} \dfrac{\beta\alpha}{(\mu+\alpha)(\mu+\varepsilon+\gamma)} & \dfrac{\beta(\mu+\alpha)}{(\mu+\alpha)(\mu+\varepsilon+\gamma)} \\ 0 & 0 \end{pmatrix}.$$

The characteristic polynomial of above matrix is

$$\lambda^2 - \frac{\beta\alpha}{(\mu+\alpha)(\mu+\varepsilon+\gamma)}\lambda = 0$$

The basic reproduction number $\mathcal{R}_0 = \max\{\lambda_1, \lambda_2\}$ is given by

$$\mathcal{R}_0 = \frac{\beta\alpha}{(\mu+\alpha)(\mu+\varepsilon+\gamma)}. \tag{8}$$

Theorem 4.1 The WFE of the projected model (1) is locally asymptomatically stable whenever $\mathcal{R}_0 < 1$
Proof. At WFE point P, the Jacobian matrix is

$$\mathsf{J} = \begin{pmatrix} -(\mu+p) & 0 & \dfrac{-\beta\mathcal{A}(\mu+\eta)}{\mu(\mu+\eta+p)} & \delta & \eta \\ 0 & -(\mu+\alpha) & \dfrac{-\beta\mathcal{A}(\mu+\eta)}{\mu(\mu+\eta+p)} & 0 & 0 \\ 0 & \alpha & -(\mu+\eta+p) & 0 & 0 \\ 0 & 0 & \gamma & -(\mu+\delta) & 0 \\ p & 0 & 0 & 0 & -(\mu+\eta) \end{pmatrix}. \tag{9}$$

Since eigen values of (9) are:

$$-(\mu+p), -(\mu+\eta+p), -(\mu+\alpha), -(\mu+\delta) \text{ and } -(\mu+\eta)$$

Hence all eigen values are negative. As a result of Routh-Hurwirtz criteria, all the eigen values of Jacobian matrix J in (9) have a negative real part. Therefore $\mathcal{R}_0 < 1$. Hence the proposed model (1) is locally asymptotically stable at equilibrium point P.

5 HU-stability

Following [36], in this section, we check out fractional-order model (1) for the global stability, within the frame of Ulam-Hyers stability criteria.
Definition 5.1[38] The system (1) is HU stable if $\exists \quad \Delta^* > 0$ and following hold true: for some ε^*
If,

$$\left| {}^{c}\mathcal{D}^{\varpi}\aleph(t) - \mathcal{H}\left(t, \aleph(t)\right)\right| \leq \varepsilon^*, \tag{10}$$

then $\exists$ a continuous function $\bar{\aleph}(t)$, which satisfy the model (1) with intial condition:

$$\aleph(0) = \bar{\aleph}(0) \tag{11}$$

such that

$$|\aleph(t) - \bar{\aleph}(t)| \leq \Delta^*\varepsilon^*. \tag{12}$$

A function $\bar{\aleph}$ is a solution of Equ. (10), if there exist $g(t) \in C[0,b]$ such that $g(0) = 0$ with the following properties.

$$|g(t)| \leq \varepsilon_1^*, \qquad \text{for} \quad t \in [0,b] \quad \text{and} \quad \varepsilon_1^* > 0$$

Lemma 5.1 The solution of the problem

$$\begin{aligned} {}^c\mathcal{D}^{\omega}\bar{\aleph}(t) &= \mathcal{H}\big(t, \bar{\aleph}(t)\big) + g(t), \\ \bar{\aleph}(0) &= \bar{\aleph}_0 \end{aligned} \tag{13}$$

satisfies the given relation

$$|\aleph(t) - \bar{\aleph}(t)| \leq \Delta^* \varepsilon^*.$$

Theorem 5.2. Consider that *Lemma*(3.1) holds. Then the model 1 will be HU stable.
Proof: For the HU stability of the problem (1). Let $\bar{\aleph}(t) \in \mathcal{X}$ be the solution of the inequality 10 and the function $\aleph(t) \in \mathcal{X}$ is a unique solution of (1) with the condition

$$\bar{\aleph}(0) = \aleph(0). \tag{14}$$

That is

$$\aleph(t) = \aleph_0 + \frac{1}{\Gamma(\omega)} \int_0^t (t-\varsigma)^{\omega-1} \mathcal{H}\big(\varsigma, \aleph(\varsigma)\big) \partial\varsigma. \tag{15}$$

Due to (14), $\bar{\aleph}(0) = \aleph(0)$, then the equ. (15) becomes

$$\aleph(t) = \bar{\aleph}_0 + \frac{1}{\Gamma(\omega)} \int_0^t (t-\varsigma)^{\omega-1} \mathcal{H}\big(\varsigma, \aleph(\varsigma)\big) \partial\varsigma.$$

$$\begin{aligned} |\bar{\aleph}(t) - \aleph(t)| &\leq |\bar{\aleph}_0 - \aleph_0| + \sup_{t\in[0,b]} \left\{ \frac{1}{\Gamma(\omega)} \int_0^t (t-\varsigma)^{\omega-1} |\mathcal{H}\big(\varsigma, \bar{\aleph}(\varsigma) - \mathcal{H}\big(\varsigma, \aleph(\varsigma)\big)| \partial\varsigma \right. \\ &\quad \left. + \frac{1}{\Gamma(\omega)} \int_0^t (t-\varsigma)^{\omega-1} |g(\varsigma)| \partial\varsigma \right\} \\ &\leq \mathcal{L}_{\mathcal{H}} \frac{(b)^{\omega}}{\Gamma(\omega+1)} \|\bar{\aleph} - \aleph\| + \frac{b^{\omega}}{\Gamma(\omega+1)} \varepsilon_1^* \| \\ &= \mathcal{L}_{\mathcal{H}} \Lambda \|\bar{\aleph} - \aleph\| + \Lambda \varepsilon_1^*, \end{aligned}$$

which implies that

$$\|\bar{\aleph} - \aleph\| \leq \frac{\Lambda \varepsilon_1^*}{1 - \mathcal{L}_{\mathcal{H}} \Lambda}.$$

Due to equ.(7), $\mathcal{L}_{\mathcal{H}} \Lambda < 1$. For $\lambda = \dfrac{\Lambda}{1 - \mathcal{L}_{\mathcal{H}} \Lambda}$,
we have

$$\|\bar{\aleph} - \aleph\| \leq \lambda \varepsilon_1^*.$$

Hence the model (1) is HU stable.

6 Numerical solution of the projected model using predictor-corrector algorithm

In this section, we find numerical solution of the model (1) in Caputo's sense using Adams type Predictor-Corrector iterative scheme [39,40]. The proposed model is defined as

$${}^c\mathcal{D}^{\omega}\aleph(t) = \mathcal{H}\big(t, \aleph(t)\big); \quad \aleph(0) = \aleph_0 \geq 0, \quad t \in [0,b], \quad 0 < \omega \leq 1. \tag{16}$$

Consider the uniform grid $\{t_n = nh;\ n = 0,1,2,\cdots,N\}$ where n and N are integers such that $h = \dfrac{b}{n}$ denotes the step size. Suppose we have already calculated the approximations $\aleph_h(t_i) \approx \aleph(t_i),\ i = 0,1,2,\cdots,n$. We calculate $\aleph_h(t_{n+1})$ using the integral equation equivalent to the Eq.(16).

$$\aleph_h(t_{n+1}) = \sum_{k=0}^{[\omega]-1} \frac{t_{n+1}^k \aleph_0^k}{k!} + \frac{h^\omega}{\Gamma(\omega+2)}\Big[\mathcal{H}\left(t_{n+1}, \aleph_h^p(t_{n+1})\right) + \sum_{i=0}^{n} p_{i,n+1}\mathcal{H}\left(t_i, \aleph_h(t_i)\right)\Big],$$

where

$$p_{i,n+1} = \begin{cases} n^{\omega+1} - (n-\omega)(n+1)^\omega, & \text{if } i = 0, \\ (n-i+2)^{\omega+1} + (n-i)^{\omega+1} - 2(n-i+1)^{\omega+1}, & \text{if } 1 \le i \le n, \\ 1, & \text{if } i = n+1. \end{cases}$$

The Predictor-formula is derived as:

$$\aleph_h^p(t_{n+1}) = \sum_{k=0}^{[\omega]-1} \frac{t_{n+1}^k}{k!} + \frac{1}{\Gamma(\omega)} \sum_{i=0}^{n} q_{i,n+1}\mathcal{H}(t_i, \aleph_h(t_i)),$$

where

$$q_{i,n+1} = \frac{h^\omega}{\omega}\left[(n-i+1)^\omega - (n-i)^\omega\right].$$

Thus the corrector formula for the projected model (1.1) is

$$\mathcal{S}_h(t_{n+1}) = \sum_{k=0}^{[\omega]-1} \frac{t_{n+1}^k \mathcal{S}_0^k}{k!} + \frac{h^\omega}{\Gamma(\omega+2)}\Big[\Psi_1\left(t_{n+1}, \mathcal{S}_h^p(t_{n+1})\right) + \sum_{i=0}^{n} p_{i,n+1}\Psi_1\left(t_i, \mathcal{S}_h(t_i)\right)\Big],$$

$$\mathcal{E}_h(t_{n+1}) = \sum_{k=0}^{[\omega]-1} \frac{t_{n+1}^k \mathcal{E}_0^k}{k!} + \frac{h^\omega}{\Gamma(\omega+2)}\Big[\Psi_3\left(t_{n+1}, \mathcal{E}_h^p(t_{n+1})\right) + \sum_{i=0}^{n} p_{i,n+1}\Psi_3\left(t_i, \mathcal{E}_h(t_i)\right)\Big],$$

$$\mathcal{I}_h(t_{n+1}) = \sum_{k=0}^{[\omega]-1} \frac{t_{n+1}^k \mathcal{I}_0^k}{k!} + \frac{h^\omega}{\Gamma(\omega+2)}\Big[\Psi_2\left(t_{n+1}, \mathcal{I}_h^p(t_{n+1})\right) + \sum_{i=0}^{n} p_{i,n+1}\Psi_2\left(t_i, I_h(t_i)\right)\Big],$$

$$\mathcal{R}_h(t_{n+1}) = \sum_{k=0}^{[\omega]-1} \frac{t_{n+1}^k R_0^k}{k!} + \frac{h^\omega}{\Gamma(\omega+2)}\Big[\Psi_4\left(t_{n+1}, \mathcal{R}_h^p(t_{n+1})\right) + \sum_{i=0}^{n} p_{i,n+1}\Psi_4\left(t_i, \mathcal{R}_h(t_i)\right)\Big],$$

$$\mathcal{V}_h(t_{n+1}) = \sum_{k=0}^{[\omega]-1} \frac{t_{n+1}^k \mathcal{V}_0^k}{k!} + \frac{h^\omega}{\Gamma(\omega+2)}\Big[\Psi_5\left(t_{n+1}, \mathcal{V}_h^p(t_{n+1})\right) + \sum_{i=0}^{n} p_{i,n+1}\Psi_5\left(t_i, \mathcal{V}_h(t_i)\right)\Big],$$

where

$$\mathcal{S}_h^p(t_{n+1}) = \sum_{k=0}^{[\omega]-1} \frac{t_{n+1}^k}{k!} + \frac{1}{\Gamma(\omega)} \sum_{i=0}^{n} q_{i,n+1}\Psi_1(t_i, \mathcal{S}_h(t_i)),$$

$$\mathcal{E}_h^p(t_{n+1}) = \sum_{k=0}^{[\omega]-1} \frac{t_{n+1}^k}{k!} + \frac{1}{\Gamma(\omega)} \sum_{i=0}^{n} q_{i,n+1}\Psi_3(t_i, \mathcal{E}_h(t_i)),$$

$$\mathcal{I}_h^p(t_{n+1}) = \sum_{k=0}^{[\omega]-1} \frac{t_{n+1}^k}{k!} + \frac{1}{\Gamma(\omega)} \sum_{i=0}^{n} q_{i,n+1}\Psi_2(t_i, \mathcal{I}_h(t_i)),$$

$$\mathcal{R}_h^p(t_{n+1}) = \sum_{k=0}^{[\omega]-1} \frac{t_{n+1}^k}{k!} + \frac{1}{\Gamma(\omega)} \sum_{i=0}^{n} q_{i,n+1}\Psi_4(t_i, \mathcal{R}_h(t_i)),$$

$$\mathcal{V}_h^p(t_{n+1}) = \sum_{k=0}^{[\omega]-1} \frac{t_{n+1}^k}{k!} + \frac{1}{\Gamma(\omega)} \sum_{i=0}^{n} q_{i,n+1}\Psi_5(t_i, \mathcal{V}_h(t_i)).$$

7 Computational discussion of the model

In this section, using variable and parameter values, we investigate the computational behavior of solutions of fractional order WSNs model. The WSNs can be utilized for a variety of objectives, including monitoring terrorist activities in remote locations and force protection. These networks, which are outfitted with suitable sensors, can detect hostile

movement, identify enemy forces, and analyze their movement and progress. Recently, WSNs is widely used in different areas such as healthcare, precision agriculture and smart cities. We check the dynamical behavior of fractional order WSNs model by using different values of fractional order and parameter values by the use of Predictor-Corrector method in sense of Caputo operator.

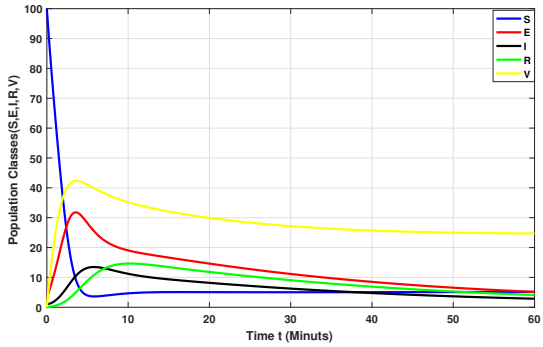

(a)

Fig. 1: A combine numerical computation of all classes for the WSNs model.

In Fig.1, Numerical plotting of combine classes, where $\mathcal{S}$ susceptible class, $\mathcal{E}$ class of exposed individual, $\mathcal{I}$ infected papulation, $\mathcal{R}$ recovered rate, $\mathcal{V}$ vaccinated size. Assuming the WSNs model's parametric parameters such, $A = 0.33,\ \mu = 0.003,\ \beta = 0.1,\ p = 0.15,\ \eta = 0.06,\ \delta = 0.3,\ \alpha = 0.25,\ \varepsilon = 0.07,\ \gamma = 0.4$ and assuming initial conditions for $\mathcal{S}(0) = 100,\ \mathcal{E}(0) = 3,\ \mathcal{I}(0) = 1,\ \mathcal{R}(0) = 0$ and $\mathcal{V}(0) = 0$. In Fig.2, Numerical plotting of susceptible

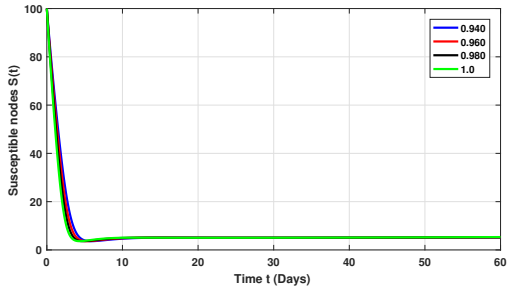

(a)

Fig. 2: Computational comparison of susceptible class with the real data in the fractional order WSNs model.

class. As the fractional order $\omega = 0.940, 0.960, 0.980$ increasing we see the effect of fractional order operator that the graph curve going close to real data. By using the parametric values in the Caputo fractional order WSNs model the parameter values, $A = 0.33,\ \mu = 0.003,\ \beta = 0.1,\ p = 0.15,\ \eta = 0.06,\ \delta = 0.3,\ \alpha = 0.25,\ \varepsilon = 0.07,\ \gamma = 0.4$ and assuming initial conditions for $\mathcal{S}(0) = 100,\ \mathcal{E}(0) = 3,\ \mathcal{I}(0) = 1,\ \mathcal{R}(0) = 0$ and $\mathcal{V}(0) = 0$. In Fig.3, Numerical plotting of exposed class. As the fractional order $\omega = 0.940, 0.960, 0.980$ increasing we see the effect of fractional order operator that the graph curve going close to real data. By using the parametric values in the Caputo fractional order WSNs model the parameter values, $A = 0.33,\ \mu = 0.003,\ \beta = 0.1,\ p = 0.15,\ \eta = 0.06,\ \delta = 0.3,\ \alpha = 0.25,\ \varepsilon = 0.07,\ \gamma = 0.4$ and assuming initial conditions for $\mathcal{S}(0) = 100,\ \mathcal{E}(0) = 3,\ \mathcal{I}(0) = 1,\ \mathcal{R}(0) = 0$ and $\mathcal{V}(0) = 0$. In Fig.4, Numerical plotting of infected class. As the fractional order $\omega = 0.940, 0.960, 0.980$ increasing we see the effect of fractional order operator that the graph curve going close to real data. By using the parametric values in the Caputo fractional order

WSNs model the parameter values, $A = 0.33,\ \mu = 0.003,\ \beta = 0.1,\ p = 0.15,\ \eta = 0.06,\ \delta = 0.3,\ \alpha = 0.25,\ \varepsilon = 0.07,\ \gamma = 0.4$ and assuming initial conditions for $\mathcal{S}(0) = 100,\ \mathcal{E}(0) = 3,\ \mathcal{I}(0) = 1,\ \mathcal{R}(0) = 0$ and $\mathcal{V}(0) = 0$. In Fig.5, Numerical plotting of recovered class. As the fractional order $\omega = 0.940, 0.960, 0.980$ increasing we see the effect of fractional order operator that the

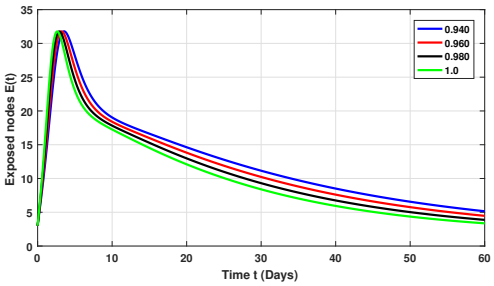

(a)

Fig. 3: Computational comparison of exposed class with the real data in the fractional order WSNs model.

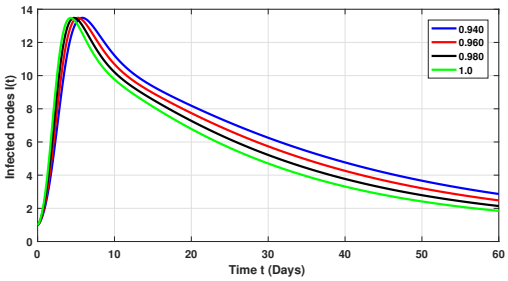

(a)

Fig. 4: Computational comparison of infected class with the real data in the fractional order WSNs model.

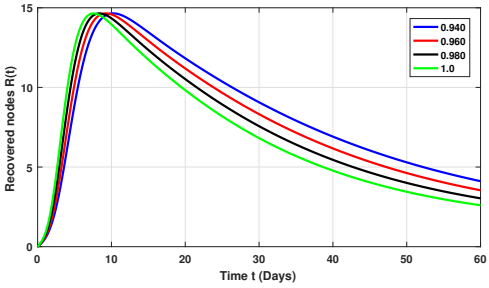

(a)

Fig. 5: Computational comparison of infected class with the real data in the fractional order WSNs model.

graph curve going close to real data. By using the parametric values in the Caputo fractional order WSNs model the parameter values, $A = 0.33,\ \ \mu = 0.003,\ \beta = 0.1,\ p = 0.15,\ \eta = 0.06,\ \delta = 0.3,\ \alpha = 0.25,\ \ \varepsilon = 0.07,\ \gamma = 0.4$ and assuming initial conditions for $\mathcal{S}(0) = 100,\ \mathcal{E}(0) = 3,\ \mathcal{I}(0) = 1,\ \mathcal{R}(0) = 0$ and $\mathcal{V}(0) = 0$

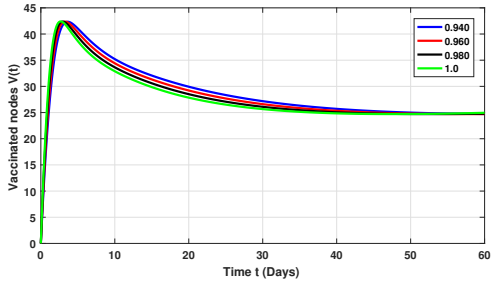

(a)

Fig. 6: Computational comparison of vaccinated class with the real data in the fractional order WSNs model.

In Fig.6, Numerical plotting of vaccinated class. As the fractional order $\omega = 0.940, 0.960, 0.980$ increasing we see the effect of fractional order operator that the graph curve going close to real data. By using the parametric values in the Caputo fractional order WSNs model the parameter values, $A = 0.33,\ \ \mu = 0.003,\ \beta = 0.1,\ p = 0.15,\ \eta = 0.06,\ \delta = 0.3,\ \alpha = 0.25,\ \ \varepsilon = 0.07,\ \gamma = 0.4$ and assuming initial conditions for $\mathcal{S}(0) = 100,\ \mathcal{E}(0) = 3,\ \mathcal{I}(0) = 1,\ \mathcal{R}(0) = 0$ and $\mathcal{V}(0) = 0$.

8 Conclusion

In this article, based on the compartmental model of biological epidemics, we consider fractional order WSNs model of worms attacking on the sensor nodes. Reproduction number is obtained to understand the spreading and fading of the worms in the sensor field. We establish that the WFE is asymptotically stable, if reproduction number $R_0 < 1$. Also the proposed model checked for the Hyres-Ulam stability. The results were simulated using Caputo operator and Corrector-Predictor method. In the above graphs, different fractional orders have been considered for the results. Furthermore, some results have been obtained regarding the EU and stability of solutions to the projected model. Finally, numerical simulations were carried out to show the dynamical behaviours of the fractional-order model using MATLAB. Study results will assist the software organization develop highly effective antivirus software to minimize attacks of malicious signals on the sensor nodes. Moreover, study results will provide users with guidelines on proper vaccination and regular use of antivirus software for preventing malicious attacks from harming their systems.

Acknowledgments

The first author would like to thanks for funding provided by the Council of Scientific and Industrial Research (CSIR)-New Delhi, India under grant no. 09/1051(0031)/2019-EMR-1.

References

[1] S. Tang and W. Li, QoS supporting and optimal energy allocation for a cluster based wireless sensor network. *Comput. Commun.***29**(13-14), 2569-2577 (2006).
[2] S. Stantiford and V. Paxton, Weaver, in: Proc. Of the 11th USENIX Security Symposium (Security '02), 2000.
[3] T.M. Chen and J-M Robert, Worm epidemics in high-speed networks. *IEEE Comput.***37**(6), 48-53 (2004).

[4] R. Pastor-Satorras and A. Vespignani, *Evolution and structure of the internet: a statistical physics approach*, Cambridge University Press, Cambridge, UK, 2004.
[5] P. Szor, *The art of computer virus research and defense: ART COMP VIRUS RES DEFENSE*. Pearson Education, Symantec Press, 2005.
[6] N. Levitt, Mobile phones: the next frontier for hackers?. *IEEE Computer***38**(4), 20-23 (2005).
[7] P. Yan, S. Liu and Yan, SEIR epidemic model with delay. *The ANZIAM J.***48**(1), 119-134 (2006).
[8] B. K. Mishra and D. K. Saini, SEIRS epidemic model with delay for transmission of malicious objects in computer network. *Appl. Math. Comput.***188**(2), 1476-1482 (2007).
[9] S. Datta and H. Wang, The effectiveness of vaccinations on the spread of email-borne computer viruses. In Canadian Conference on Electrical and Computer Engineering, 2005(2005), 219-223.
[10] C.C. Zou, W. Gong and D. Towsley, Worm propagation modeling and analysis under dynamic quarantine defense. In Proceedings of the 2003 ACM workshop on Rapid Malcode, 2003(2003),(51-60).
[11] D. Moore, C. Shannon, G.M. Voelker and S. Savage, Internet quarantine: requirements for containing self-propagating code. In IEEE INFOCOM 2003. Twenty-second Annual Joint Conference of the IEEE Computer and Communications Societies (IEEE Cat. No. 03CH37428) (Vol. 3). IEEE, 1901-1910.
[12] B. K. Mishra and N. Jha, Fixed period of temporary immunity after run of anti-malicious software on computer nodes. *Appl. Math. Comput.***190**(2), 1207-1212 (2007).
[13] T. Chen and N. Jamil, Effectiveness of quarantine in worm epidemics, in: IEEE International Conference on Communications 2006, IEEE, 2006, 2142-2147.
[14] N. Madar, T. Kalisky, R. Cohen, D. Ben Avraham and S. Havlin, Immunization and epidemic dynamics in complex networks. *Eur. Phys. J. B***38**(2), 269-276 (2004).
[15] T. Wang, Q. Wu, S. Wen, Y. Cai, H. Tian, H., Chen and B. Wang, Propagation modeling and defending of a mobile sensor worm in wireless sensor and actuator networks. *Sensors***139**, 1-17 (2017).
[16] A. Singh, A. K. Awasthi, K. Singh and P. K. Srivastava, Modeling and analysis of worm propagation in wireless sensor networks. *Wirel. Pers. Commun.***98**(3), 2535-2551 (2018).
[17] S. Misra, R. Singh and S. V. Mohan, Information warfare-worthy jamming attack detection mechanism for wireless sensor networks using a fuzzy inference system. *Sensors***10**(4), 3444-3479 (2010).
[18] B. K. Mishra and N. Keshri, Stability analysis of a predator–prey model in wireless sensor network, *Int. J. Comp. Math.***91**(5), 928-943 (2013).
[19] Y. Yao, C. Sheng, Q. Fu, H. Liu and D. Wang, A propagation model with defensive measures for PLC-PC worms in industrial networks. *Appl. Math. Modell.***69**, 696-713 (2019).
[20] Z. Zhang, R. K. Upadhyay, D. Bi and R. Wei, Stability and hopf bifurcation of a delayed epidemic model of computer virus with impact of antivirus software. *Disc. Dyn. Nat. Soc.* **2018**, 1-18 (2018).
[21] S. Muthukrishnan, S. Muthukumar and V. Chinnadurai, Optimal control of malware spreading model with tracing and patching in wireless sensor networks. *Wirel. Pers. Commun.***117**(3), 2061-2083 (2021).
[22] L. Jiang, Q. Xu, H. Pan, Y. Dai and J. Tong, Virus Propagation in Wireless Sensor Networks with Media Access Control Mechanism. *Secur. Commun. Netw.***2020**, 1-11 (2020).
[23] D. Ganeshan and T. S. Kavitha, Analytical solution of the Effect of awareness program by media on the spread of an infectious disease by homotopy perturbation method. *Tamkang J. Math.***51**(4), 333-347 (2020).
[24] E. Ilhan, Fractional approach for model of network access control using efficient method. *Balıkesir Üniv. Fen Bil. Enst. Derg.***23**(2), 732-747 (2021).
[25] G. Liu, J. Chen, Z. Liang, Z. Peng and J. Li, Dynamical analysis and optimal control for a SEIR model based on virus mutation in WSNs. *Math.***929**(9), 1-16 (2021).
[26] N. P. Dong, H. V. Long and N. L. Giang, The fuzzy fractional SIQR model of computer virus propagation in wireless sensor network using Caputo Atangana–Baleanu derivatives. *Fuzzy Set. Sys.*, (2021).
[27] A. Devi, A. Kumar, D. Baleanu and A. Khan, On stability analysis and existence of positive solutions for a general non-linear fractional differential equations. *Adv. Differ. Equ.***2020**(1), 1-16 (2020).
[28] A. Devi, A. Kumar, T. Abdeljawad and A. Khan, Existence and stability analysis of solutions for fractional Langevin equation with nonlocal integral and anti-periodic type boundary conditions. Fract.**28**, 2040006-1-2040006-12 (2020).
[29] A. Devi and A. Kumar, Existence of solutions for fractional Langevin equation involving generalized Caputo derivative with periodic boundary conditions. *AIP Confer. Proc.***2214**, 020026-1-020026-10 (2020).
[30] A. Khan, J. F. Gómez-Aguilar, T. S. Khan and H. Khan, Stability analysis and numerical solutions of fractional order HIV/AIDS model. *Chaos Soliton. Fract.***122**, 119-128 (2019).
[31] H. Khan, J. F. Gómez-Aguilar, A. Alkhazzan and A. Khan, A fractional order HIV-TB coinfection model with nonsingular Mittag-Leffler Law. *Math. Meth. Appl. Sci.***43**, 3786-3806 (2020).
[32] S. Ahmad, A. Ullah, Q. M. Al-Mdallal, H. Khan, K. Shah and A. Khan, Fractional order mathematical modeling of COVID-19 transmission. *Chaos Soliton. Fract.***139**, 1-10 (2020).
[33] S. Awasthi, N. Kumar and P. K. Srivastava, An epidemic model to analyze the dynamics of malware propagation in rechargeable wireless sensor network. *J. Disc. Math. Sci. Crypt.***24**(5), 1529-1543 (2021).
[34] I. Podlubny, *Fractional differential equations*. vol. 198. Academic Press, Son Diego, 1998.

[35] A. A. Kilbas, H. M. Srivastava and J. J. Trujillo, *Theory and applications of fractional differential equations*. vol. 204. Elsevier Science Limited (2006).
[36] Z. M. Odibat and N. T. Shawagfeh, Generalized Taylor's formula *Appl. Math. Comput.* **186**(1)(2007), 286-293.
[37] M. A. Krasnoselsky, Two remarks on the method of successive approximation. *Uspekhi Math. Nauk*, **10**(1955), 123-127.
[38] D. H. Hyers, On the stability of the linear functional equations. *Proc.Nat.Acad.Sci.* **27**(4), 222-224 (1941).
[39] K. Diethelm, N. J. Ford and A. D. Freed, Detailed error analysis for a fractional Adams method. *Numer. Algor.* **36**(1) 31-52 (2004).
[40] K. Diethelm, N. J. Ford and A. D. Freed, A predictor-corrector approach for the numerical solution of fractional differential equations. *Nonlin. Dyn.* **29**(1) 3-22 (2002).